ELSEVIER

Thermochimica Acta 304/305 (1997) 317–334

thermochimica acta

Modulated temperature differential scanning calorimetry: Cure, vitrification, and devitrification of thermosetting systems

G. Van Assche, A. Van Hemelrijck, H. Rahier, B. Van Mele*

Department of Physical Chemistry and Polymer Science, Vrije Universiteit Brussel, Pleinlaan 2, 1050 Brussels, Belgium

Received 6 August 1996; accepted 4 April 1997

Abstract

Vitrification of a reacting thermosetting system occurs when its glass transition temperature, T_g, rises to the reaction temperature, T. This phenomenon can occur in both isothermal and non-isothermal conditions, depending on the temperatures or heating rates used, the reactivity of the system, and the evolution of T_g with conversion. After vitrification, the reaction proceeds in mobility-restricted conditions. In non-isothermal experiments devitrification is observed when the reaction temperature again surpasses T_g of the vitrified resin.

The cure process of two epoxy thermosetting systems and an inorganic polymer glass has been studied using modulated temperature differential scanning calorimetry (MTDSC). A normalized mobility factor, which is directly based on the experimental heat capacity evolution, is proposed. For both organic resins, it is shown that the points for which this mobility factor equals 0.5 can be used to quantify vitrification and devitrification. Preliminary results indicate a relation between the evolution of the heat flow phase and the chemorheological transformations.

The mobility factor derived from the heat capacity is compared to a normalized diffusion factor calculated using the non-reversing heat flow and chemical kinetics modelling. For the organic resins studied, both factors coincide. Therefore, the mobility factor can be used as a direct measurement of the change in the rate of reaction due to mobility restrictions when T_g of the reacting system approaches T.

Isothermal and non-isothermal MTDSC experiments enable the reaction mechanism, the vitrification and devitrification process, and models for diffusion control to be studied, and temperature–time transformation or continuous–heating transformation diagrams for improved thermoset processing conditions to be developed. © 1997 Elsevier Science B.V.

Keywords: Devitrification; Diffusion control; Modulated temperature differential scanning calorimetry; Thermosetting polymer; Vitrification

1. Introduction

The network formation in thermosetting polymers has been studied extensively in the past. Thermal analysis techniques, and especially differential scanning calorimetry (DSC), have often been used to study reaction kinetics and the evolution of the glass transition temperature, T_g [1]. Modulated temperature differential scanning calorimetry (MTDSC) is a renovating thermal analysis technique [2–6] that opens new ways for material characterization by thermal analysis. An important advantage of MTDSC for studying thermosetting systems is that it allows a

*Corresponding author. Tel.: +32-(0)2-629.3276; fax: +32-(0)2-629.3278; e-mail: bvmele@vnet3.vub.ac.be.

PII S0040-6031(97)00175-5

simultaneous characterization of the chemical reactions and the vitrification and devitrification processes of the reacting polymer [7,8].

In two earlier publications, isothermal [7] and non-isothermal [8] cure were discussed. To illustrate the abilities of MTDSC, an amine-cured and an anhydride-cured epoxy resin, and a low-temperature inorganic polymer glass [9,10] were chosen. In this article, results are presented for both isothermal and non-isothermal cure experiments. In addition to results published earlier [7,8], results for other reaction conditions will be presented, the effect of the heating rate will be discussed, and preliminary results on the evolution of the heat flow phase lag during isothermal and non-isothermal cure will be shown.

1.1. Cure, vitrification and rate of reaction

The cure of thermosetting materials generally involves the transformation of low molecular weight liquids to amorphous networks with infinite molecular weight by means of exothermic chemical reactions. First of all the molecular weight starts increasing and branching occurs. At a certain conversion gelation takes place and a non-soluble gel-fraction is formed. Vitrification of a thermosetting system occurs when its glass transition temperature rises to the reaction temperature, T. Upon vitrification, the material transforms from a liquid or rubbery state to a glassy state. For organic systems, the attendant reduction in segmental mobility leads to a marked decrease in rate of reaction, as the reaction becomes diffusion or mobility-controlled [7,8,11–13]. Depending on the thermosetting system (its reactivity and its evolution of T_g with reaction conversion, x) and the temperature program (the isothermal temperature, T_{iso}, or the heating rate employed) vitrification can occur in both isothermal and non-isothermal experiments [7,8,14,15]. In isothermal conditions, the reaction can proceed until T_g exceeds the cure temperature to the point where all chain movement (cooperative motion) ceases, and the reaction stops due to the absence of segmental mobility (T_g approximately 50°C above T_{iso}, depending on the reacting system) [12]. This leads to a final conversion lower than unity in isothermal diffusion-controlled conditions [7,12].

1.2. Devitrification of a vitrified cure state in non-isothermal conditions

In a non-isothermal experiment, T_g can rise up to the reaction temperature if the rate of increase in T_g (due to reaction) is higher than the heating rate. Thus, factors favouring the occurrence of vitrification in non-isothermal conditions are: low heating rates, highly reactive systems, and an important variation of T_g with conversion. Upon vitrification, the rate of reaction decreases due to mobility restrictions. In the glassy state, the reaction continues at a lower rate. However, it should be noted that during this diffusion controlled cure, conversion and T_g sometimes rise substantially [8]. While the temperature further increases at a constant heating rate, the conversion nears completion and T_g nears the glass transition temperature of the fully cured network, $T_{g\infty}$. So, the rate of reaction, and also the rate of increase in T_g, will drop further, allowing the reaction temperature to surpass T_g again. This non-isothermal transformation of the glassy state to a liquid or rubbery state, called devitrification, is a phenomenon that cannot occur in isothermal experiments (unless degradation of the polymer network occurs [13,16]). It is comparable with the glass transition observed upon heating a partially reacted (or unreacted) thermosetting system.

1.3. Experimental characterization of the curing process

The previously mentioned chemorheological changes when curing thermosetting materials can be rationalized using the isothermal temperature–time transformation (TTT) cure diagram [13,15,16], the non-isothermal continuous-heating transformation (CHT) diagram [14,15], or related diagrams [17]. The state of the material is governed by chemical conversion and temperature. Knowledge of the rate of cure, its dependence on temperature and conversion, and the influence of the chemorheological changes is important for predicting the course of the reaction for a certain thermal treatment.

For a complete quantification of TTT and CHT diagrams, one has to describe the entire curing process for conditions where the chemical reactions and the rheological changes are coupled. Therefore, a simul-

taneous measurement of both the evolution of conversion and, for example, the evolution of the vitrification process is very useful.

Mostly, the chemorheological changes were characterized using, for example, dynamic mechanical analysis [10] or torsional braid analysis [14–16], dielectric thermal analysis [18–20], rheometry and dynamic rheometry [21,22], gelbench experiments, and Soxhlet extraction [23]. However, these techniques give no simultaneous quantitative information about the evolution of the conversion or rate of conversion with time and temperature. Conventional DSC can be employed to determine the evolution and rate of conversion as a function of time and temperature, but the chemorheological changes can only be observed indirectly (from their influence on the rate of reaction). Thus, from a single DSC experiment it is impossible, firstly, to determine whether such a phenomenon of changed reaction rate is due to rheological transformation or to complex reaction kinetics, and secondly, to quantify it properly.

Cassettari et al. [24,25] studied the cure of epoxy-amine resins using a differential microcalorimeter especially designed to enable the simultaneous measurement of heat capacity and the rate of enthalpy release. The instrument allows only for isothermal measurements.

In a single, isothermal or non-isothermal, MTDSC experiment, the evolution of the rate of reaction can be followed quantitatively in the non-reversing heat flow signal, while vitrification and devitrification can be observed quantitatively in the heat capacity signal [7,8]. Thus, this technique offers a great opportunity for studying the coupled chemical reactions and vitrification–devitrification processes of thermosetting systems [7,8].

2. Experimental

2.1. Epoxy resins

The amine-cured epoxy consisted of a tetrafunctional epoxy (MY 720) combined with a stoichiometric amount of tetrafunctional amine hardener (HY 2954), with an epoxy equivalent weight (EEW) and amine equivalent weight of 125 g eq^{-1} and 59.5 g eq^{-1} respectively. The anhydride-cured epoxy contained a bifunctional DGEBA-type epoxy (LY 556, EEW=183–192 g eq^{-1}, n=0.13), a tetrafunctional anhydride hardener (HY 917, anhydride equivalent weight=166 g eq^{-1}), and an accelerator (DY 070), mixed in an LY 556/HY 917/DY 070 weight ratio of 100/90/1, resulting in a stoichiometric mixture.

The chemical structure of the reactants is given in Fig. 1. All components are from Ciba-Geigy and were used without purification. The prescribed amounts of the components were added to a weighed amount of epoxy. A magnetic stirrer was employed at room temperature to obtain a homogeneous mixture. The recipient was sealed hermetically and stored at −20°C.

2.2. Inorganic polymer glass

The inorganic polymer glass (IPG) is an amorphous aluminosilicate formed by a low-temperature reaction of an alkaline sodium silicate solution with a dehydroxylated clay (metakaolinite), defined as $(Na_2O)(SiO_2)_{1.4}(H_2O)_X$ ('X' stands for the bound water in the solution) and $(Al_2O_3)(SiO_2)_2(H_2O)_{0.05}$ respectively. The molar mass ratios of SiO_2/Na_2O, H_2O/Na_2O for the sodium silicate solution, and of silicate/metakaolinite, equaled 1.4, 10, and 1.0, respectively. The overall reaction can be written as

$$(Na_2O)(SiO_2)_{1.4}(H_2O)_X + (Al_2O_3)(SiO_2)_2(H_2O)_{0.05} \xrightarrow{\text{aq.}(\leq 100^\circ C)} (Na_2O)(Al_2O_3)(SiO_2)_{3.4}(H_2O)_Z$$

where Z is about 0.4 [9]. The materials and the sample preparation are described in Ref. [9].

2.3. Analytical techniques: Instrumentation, calibration and experimental procedures

Modulated temperature isothermal and non-isothermal experiments were performed on a TA Instruments 2920 DSC with MDSC™ option and equipped with two cooling systems: a refrigerated cooling system (RCS) or a liquid nitrogen cooling accessory (LNCA). The RCS enables one to employ very long measurement times, which is useful for isothermal experiments at lower temperatures (low rate of reaction) and for very slow heating experiments. The LNCA allows experiments to be started at −150°C compared to −70°C for the RCS.

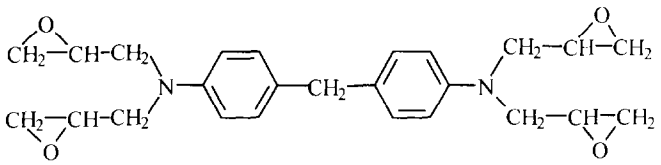

N,N,N',N'-tetraglycidyl-4,4'-diaminodiphenylmethane (MY 720)

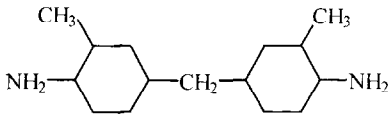

3,3'-dimethyl-4,4'-diaminodicyclohexylmethane (HY 2954)

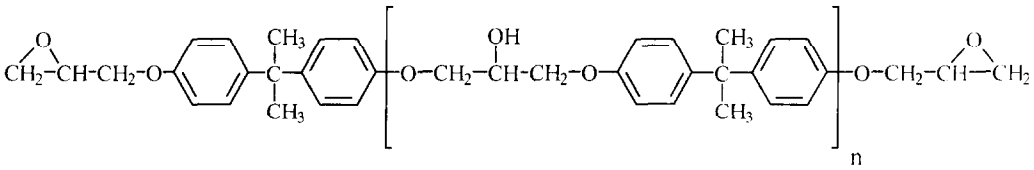

diglycidyl ether of bisphenol A (LY 556)

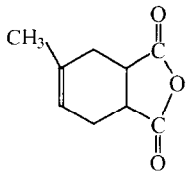

methyltetrahydrophthalic anhydride (HY 917)

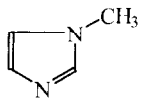

1-methyl imidazole (DY 070)

Fig. 1. Chemical structure of the organic reactants.

Helium was used as a purge gas (25 ml min^{-1}). Temperature was calibrated using cyclohexane and indium. Indium was used for the enthalpy calibration. The heat capacity signal was calibrated at a single point. For the organic systems, a linear polyethylene reference material NIST SRM 1475 [26] at 150°C ($C_p = 2.57\ J\ g^{-1}\ K^{-1}$ [27]) was used. For the IPG the heat capacity was calibrated with a 1/1 mixture by weight of kaolinite KGa-1 ($C_p = 0.956\ J\ g^{-1}\ K^{-1}$ [28]) and water ($C_p = 4.180\ J\ g^{-1}\ K^{-1}$) at 25°C.

For the calibrations the same pan type, sample heat capacity (sample weight times specific heat capacity), and period were used as in the corresponding experiments. The experimental error on the heat capacity values cited was about 2%. For more accurate results, especially at temperatures below −50°C, a dynamic heat capacity calibration procedure was applied (see Section 3.9.1).

For the organic systems, hermetic aluminium pans (TA Instruments) were used. The sample weight was 10 to 20 mg. Quasi-isothermal experiments with a modulation amplitude of 0.5°C and a 60 s-period were performed at temperatures ranging from 60°C to 120°C. Non-isothermal experiments were performed at heating rates of 0.2°C min^{-1} to 2.5°C min^{-1}, with a modulation amplitude of 0.10°C to 0.30°C and a 60 s-period. When appropriate, a second heating of the fully reacted sample was made, under the same conditions, to determine the evolution of the heat capacity of the fully cured network.

For partial cure reactions, the experiment was halted at a predetermined time (or temperature). The glass transition temperature, T_g, and the residual cure were measured in a second heating from −50°C to 275°C at 2.5°C min^{-1} with a 0.3°C per 60 s modulation. The total reaction enthalpy, ΔH_{tot}, measured in a conventional DSC experiment at 10°C min^{-1} amounts to −530 J g^{-1} and −335 J g^{-1} for the epoxy-amine and anhydride systems respectively.

For kinetic modelling, MTDSC and conventional DSC experiments at multiple isothermal temperatures, ranging from 60°C to 120°C, and at multiple scan rates, ranging from 2.5°C min^{-1} to 15°C min^{-1}, were performed.

For the IPG system, reusable high pressure stainless steel sample pans (Perkin Elmer) were used, withstanding an internal pressure of 150 atm. The pan weights were about 630 mg and were matched on sample and reference sides. It was necessary to use these high pressure pans because free water is present during the reaction and temperature is increased up to 300°C in non-isothermal experiments. For quasi-isothermal experiments, the sample was scanned at 20°C min^{-1} from 20°C to the isothermal temperature where a modulation of 0.5°C and 100 s was superimposed. The total reaction enthalpy measured for a heating at 5°C min^{-1} in conventional DSC equals −230 J g^{-1} [9].

A 0.5°C amplitude was chosen for the quasi-isothermal experiments to achieve sufficient sensitivity for the heat capacity measurement. For the IPG experiments the period was increased to 100 s because of the higher thermal mass of the high pressure pans.

3. Results and discussion

3.1. Isothermal vitrification

Fig. 2 shows the non-reversing heat flow and the heat capacity as a function of reaction time for the quasi-isothermal cure of the epoxy-anhydride resin at 80°C for 600 min. The reaction exotherm obeys an autocatalytic behaviour: the heat flow increases at first and passes through a maximum. The heat capacity C_p first decreases slightly. Subsequently a stepwise decrease in C_p is observed, simultaneously with a sharp decrease in heat flow. The heat capacity change equals 0.38 J g^{-1} K^{-1}. The time at half of the change between the heat capacity of the liquid state and the glassy state, $t_{1/2\Delta C_p}$, equals 248 min. The glass transition temperature at this instant, measured in a partial cure experiment, amounts to 80°C. Therefore $t_{1/2\Delta C_p}$ obtained in an MTDSC experiment can be used to quantify the time of vitrification. This time can be interpreted as the time at which half of the material has transformed to the glassy state (on the time scale of the modulation).

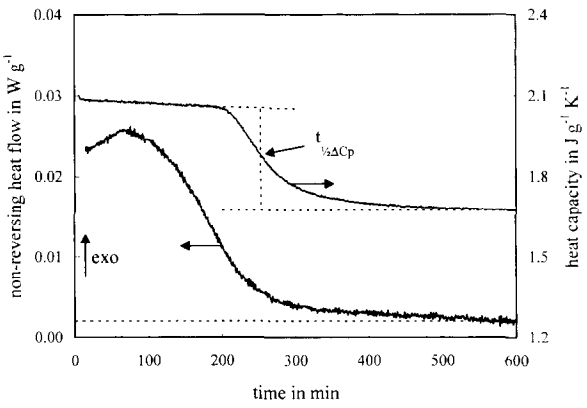

Fig. 2. Non-reversing heat flow and heat capacity C_p for the quasi-isothermal cure of the epoxy-anhydride at 80°C with a 0.5°C per 60 s modulation. $t_{1/2\Delta C_p}$ is the time at half of the decrease in heat capacity.

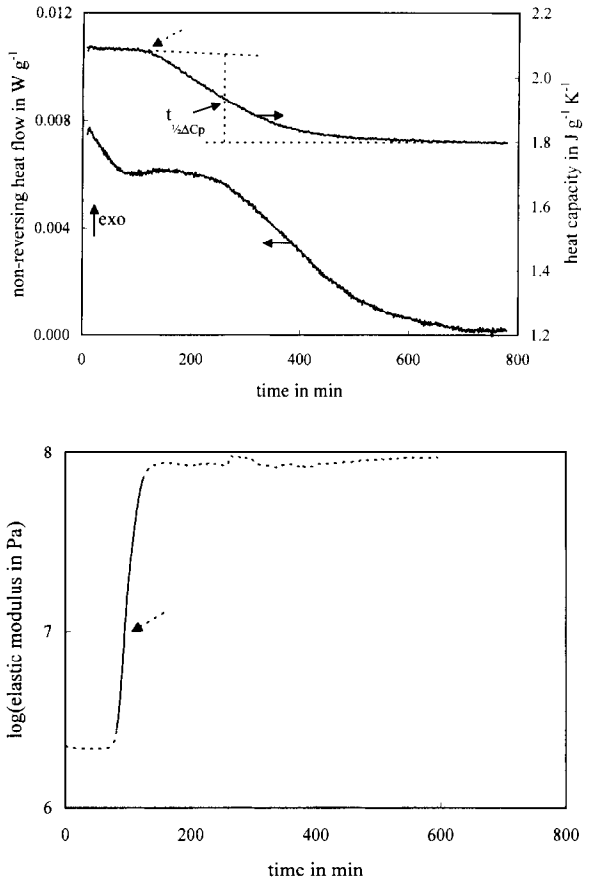

Fig. 3. (a) Non-reversing heat flow and heat capacity C_p for the quasi-isothermal cure of the inorganic polymer glass at 35°C with a 0.5°C per 100 s modulation [7]. The dashed arrow points to the onset of vitrification.(b) Evolution of the elastic modulus for the quasi-isothermal cure of the inorganic polymer glass at 35°C, measured using dynamic mechanical analysis. The levels reached at both plateaus (- - - -) are due to the experimental set-up. The dashed arrow points to the onset of vitrification.

The low-temperature synthesis of the amorphous aluminosilicate was studied quasi-isothermally at 35°C for 800 min. The reaction exotherm shows a typical behaviour with the maximum rate of reaction at the start of the experiment followed by a shoulder of more or less constant rate of reaction (Fig. 3(a)). The heat capacity remains nearly constant up to 20% conversion, then a gradual decrease is observed resulting in a ΔC_p equal to 0.27 J g^{-1} K^{-1} with $t_{1/2\Delta C_p}$ equal to 245 min. The rate of reaction stays more or less the same over the first half of the change in C_p and decreases slowly over the second half. At the end of the reaction exotherm a conversion of 75% is reached (based on a total reaction enthalpy of −230 J g^{-1}). A second heating shows a residual exotherm (−57 J g^{-1}) setting in at about 175°C and with a maximum at 238°C. In this second heating no glass transition is observed before the onset of the residual reaction exotherm (where T_g starts increasing again), leading to the conclusion that T_g has risen to at least 175°C during the isothermal cure at 35°C [9,10]. Since the residual cure reaction already starts while in the glassy state it is impossible to measure the T_g after isothermal cure in a second heating.

Fig. 3(b) shows for the reaction of the IPG at 35°C the evolution of the elastic modulus measured with dynamic mechanical analysis (DMA). A description and discussion of the experimental set-up can be found in Ref. [10]. The onset of the decrease in C_p measured with MTDSC corresponds to the onset of vitrification defined by the strong rise in elastic modulus found in DMA [10]. This indicates, once again the stepwise decrease in C_p describing the vitrification process, so that $t_{1/2\Delta C_p}$ can be used as a measure for the vitrification time.

3.2. *Non-isothermal (de)vitrification of the organic systems*

Fig. 4(a) shows the non-reversing heat flow and heat capacity as a function of temperature for the cure of the epoxy-anhydride at a heating rate of 0.2°C min^{-1}. The heat capacity evolution for the completely cured resin, measured using identical conditions, is also shown. The reaction exotherm shows a maximum around 90°C, and is followed by a shoulder of more or less constant heat flow. The shoulder's height is 7% of the peak height or approx. 50 μW, and it spans a temperature interval of 40°C. In the heat capacity curve of the first heating, three transitions are observed. T_{go} of the uncured resin equals −37°C, with a $\Delta C_p(T_{go})$ of 0.49 J g^{-1} K^{-1}. The second transition, a decrease in C_p of 0.28 J g^{-1} K^{-1}, occurs at the instant the heat flow decreases. Near the end of the heat flow shoulder, C_p increases again with a ΔC_p of 0.23 J g^{-1} K^{-1}. In between the transitions, C_p rises slowly with temperature. In a second heating, $T_{g\infty}$ of the fully cured network amounts to 135°C, with a ΔC_p of 0.28 J g^{-1} K^{-1}. Measured against this second heating reference line, the temperatures at half of the heat

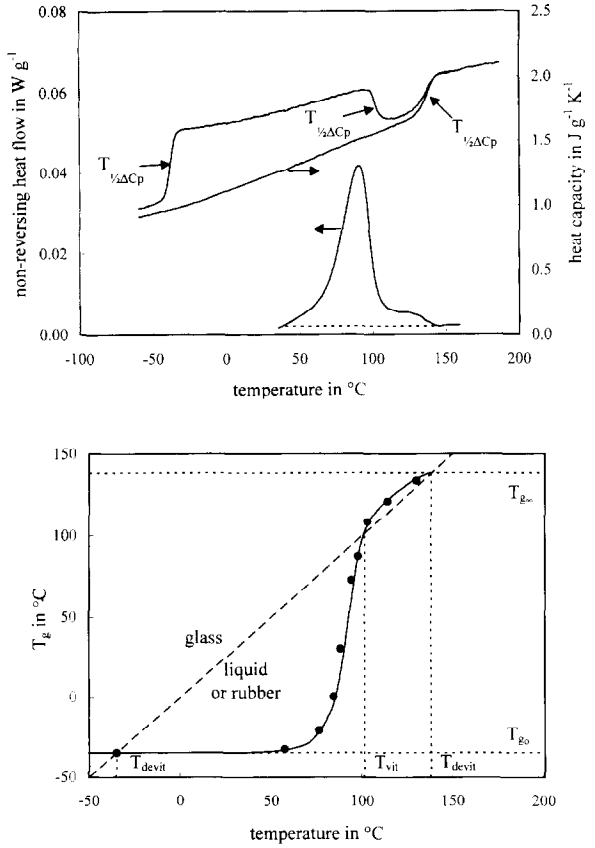

Fig. 4. (a) Non-reversing heat flow and heat capacity for the non-isothermal cure of the epoxy-anhydride and heat capacity for the fully cured material, at 0.2°C min^{-1} with a 0.15°C per 60 s modulation. $T_{1/2\Delta C_p}$ is the temperature at half of the step in heat capacity.(b) Evolution of the glass transition temperature, T_g, measured in partial cure experiments for the non-isothermal cure of the epoxy-anhydride at 0.2°C min^{-1} with a 0.15°C per 60 s modulation. The line linking the points is a guide to the eye only.

capacity difference, $T_{1/2\Delta C_p}$, equal −37°C (T_{go}), 104°C and 131°C, respectively.

The evolution of T_g with reaction temperature for the experimental conditions of Fig. 4(a) was determined by residual cure experiments for a number of partially reacted samples (Fig. 4(b)). Initially the material is in the glassy state, and devitrification occurs for the first time when T reaches T_{go}. The reaction starts at about 25°C. As the rate of reaction increases, T_g rises more rapidly. At the heat flow maximum T_g increases with a rate of 2°C min^{-1}, or 10 times faster than the applied heating rate of 0.2°C min^{-1}. Vitrification occurs when T_g surpasses T at 101°C (T_{vit}). The attendant decrease in segmental mobility causes a decrease in the rate of reaction, and the T_g curve runs more or less parallel with T. In this zone, the rate of reaction is controlled by the heating rate. A maximum difference $T_g - T$ of 7°C is reached. As the reaction continues, T_g increases more slowly because the conversion nears completion (T_g nears $T_{g\infty}$), and devitrification occurs at a temperature of approx. 135°C (T_{devit}). Comparison of the evolutions of C_p and T_g (Fig. 4(a,b)) clearly shows that the three transitions in heat capacity, characterized by the temperatures $T_{1/2\Delta C_p}$, subsequently correspond to the devitrification, vitrification and devitrification processes. Therefore, the three $T_{1/2\Delta C_p}$ points obtained in a single non-isothermal MTDSC experiment can be used to quantify vitrification and devitrification.

The results for the amine-cured epoxy at a heating rate of 1°C min^{-1} are shown in Fig. 5. The overall picture is similar to the result for the epoxy-anhydride (Fig. 4(a)). T_{go} equals −23°C. The non-reversing heat flow passes through a maximum at 100°C, and then decreases sharply. Simultaneously, a sharp decrease in heat capacity occurs. For a partial cure experiment stopped at this point, a small peak in C_p near 105°C is observed in the second heating. The onset of the residual reaction exotherm is 90°C. Considering the high reactivity of this resin and the results for a heating rate of 0.2°C min^{-1} [8], one can conclude that before a complete devitrification can occur, T_g starts increasing

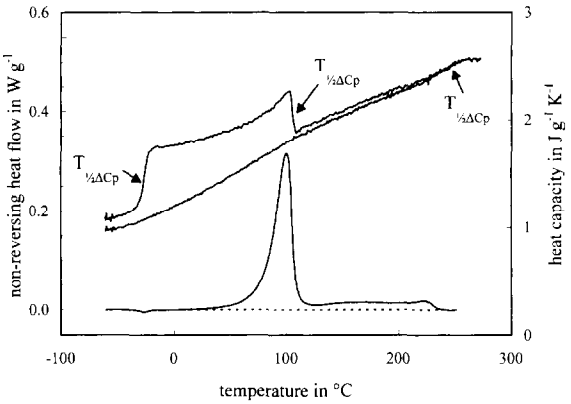

Fig. 5. Non-reversing heat flow and heat capacity for the non-isothermal cure of the epoxy-amine and heat capacity for the fully cured material, at 1°C min^{-1} with a 0.15°C per 60 s modulation. $T_{1/2\Delta C_p}$ is the temperature at half of the step in heat capacity.

again due to the residual reaction, thus causing an immediate revitrification. Bearing this in mind, the results point to the occurrence of vitrification at the instant that heat flow and heat capacity decrease in Fig. 5. Between 125°C and 250°C, a temperature interval of 125°C, a small heat flow is still observed (80 to 200 μW; Fig. 5). A second (low) maximum is attained around 220°C. Then the heat flow decreases to reach the baseline level near 250°C. Over the 125°C wide interval, C_p of the curing network (first heating) and C_p of the fully cured, vitrified resin (second heating) slowly converge. The first and second heating both show a small step in C_p (0.1 J g^{-1} K^{-1}) ending at approx. 255°C. Since the reaction is completed near 250°C, this change in C_p corresponds most probably to devitrification. Neither this transition nor $T_{g\infty}$ can be determined unambiguously because the step change in heat capacity is small, and because degradation of the polymer network becomes prominent at 275°C. The smallness of $\Delta C_p(T_{g\infty})$ is due to the high crosslink density of the fully cured resin, so that little mobility will be freed beyond $T_{g\infty}$ due to the restrictions of the tight network [29]. The higher final crosslink density for the tetrafunctional epoxy-amine (in comparison with the bifunctional epoxy-anhydride), is reflected in a higher $T_{g\infty}$ (approx. 250°C) and a smaller $\Delta C_p(T_{g\infty})$.

3.3. Effect of heating rate

Fig. 6(a,b) shows the influence of the heating rate on the vitrification–devitrification behaviour of the anhydride and amine-cured epoxy, respectively. For the epoxy-anhydride system, no vitrification is observed at heating rates of 1°C min^{-1} or higher. On the contrary, for the epoxy-amine system even at a heating rate of 2.5°C min^{-1} a strong vitrification can be seen. The heating rate has to be even higher than 20°C min^{-1} to avoid vitrification [30]. This indicates that attention needs to be paid when using non-isothermal experiments to study the reaction kinetics: the reaction does not occur *de facto* in chemically controlled conditions, even at higher heating rates.

For both systems the vitrification temperature is higher for higher heating rates. At a higher heating rate it takes less time to reach a certain temperature. Consequently, a lower conversion and T_g are attained

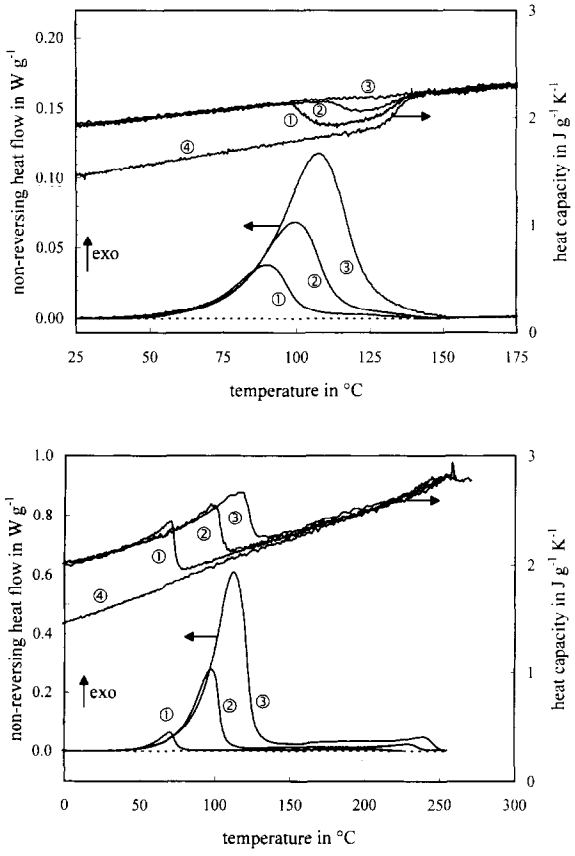

Fig. 6. (a) Non-reversing heat flow and heat capacity for the non-isothermal cure of the epoxy-anhydride at 0.2 (1), 0.4 (2), and 0.7°C min^{-1} (3), and heat capacity for the fully cured material (4), with a 60 s modulation.(b) Non-reversing heat flow and heat capacity for the non-isothermal cure of the epoxy-amine at 0.2 (1), 1 (2), and 2.5°C min^{-1} (3), and heat capacity for the fully cured material (4), with a 60 s modulation.

at that temperature and vitrification is shifted to higher temperatures. This shift is obviously limited by $T_{g\infty}$, the devitrification temperature of the fully cured resin. For the epoxy-anhydride, when the heating rate is increased, the minimum level of C_p in between T_{vit} and T_{devit} is closer to C_p of the liquid state (Fig. 6(a)). This implies that less mobility is frozen in and that a smaller fraction of the material transforms to the glassy state. For the amine-cured epoxy, at 1°C min^{-1} the interval between vitrification and devitrification is approx. 125°C wide. In this interval, C_p converges to C_p of the fully cured (glassy) network (Fig. 6(b)), indicating that the material vitrifies almost completely.

3.4. Influence of reaction conversion on heat capacity

When the heat capacities of reactants and products differ, a reaction induces a gradual change in heat capacity with reaction conversion, ΔC_{pr}. For the epoxy-anhydride, the influence of reaction conversion on heat capacity is small: up to vitrification, which occurs at a conversion of more than 80% in an isothermal experiment at 80°C, C_p only slightly decreases (Fig. 2). However, for the epoxy-amine system the influence is more important. This can be seen from the linear rise in heat capacity (0.11 J g^{-1} K^{-1}) from 0% up to 40% conversion (onset of vitrification) in an isothermal experiment at 70°C [7], from the small peak in heat capacity coinciding with the reaction exotherm in non-isothermal experiments (Fig. 5 and Ref. [8]), and from the difference in heat capacity for the vitrified state of the uncured and the fully cured resin (compare the first and second heating below T_{go} in Fig. 5). Moreover, the heat capacities for zero and full conversion are not simply shifted, their temperature-dependence is also different. This can, for example, be seen from a different evolution of C_p for the liquid or rubbery states before vitrification and after devitrification (Fig. 4a and Fig. 5). Note that the curvature of the heat capacity evolution for both uncured and cured materials, is at least partly reduced when the heat capacity is calibrated over the entire temperature range, as shown in Fig. 7. The dynamic heat capacity calibration is more elaborately discussed in Section 3.9.1.

Due to change in the heat capacity by reaction, ΔC_{pr}, the total reaction enthalpy, ΔH_{tot}, depends on the average temperature of the experiment. For the epoxy-amine system, ΔC_{pr} is below 0.2 J g^{-1} K^{-1} and the maximum difference between the mean temperatures of the experiments is approx. 100°C. This results in a maximum difference in ΔH_{tot} between two experiments of 20 J g^{-1}, or less than 4% when compared to the value of −530 J g^{-1} for ΔH_{tot}. For the epoxy-anhydride the influence on ΔH_{tot} is much smaller because both ΔC_{pr} and the temperature range are smaller. So, for the vast majority of experiments this correction on ΔH_{tot} due to ΔC_{pr} is negligible compared to deviations on ΔH_{tot} between individual experiments (e.g. due to variations in mixing ratios of components and to minor amounts of moisture).

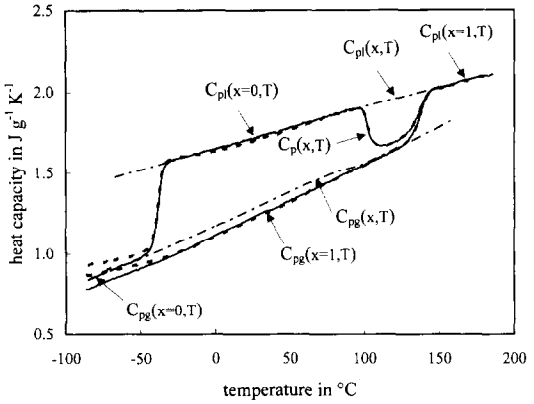

Fig. 7. Heat capacity profiles versus temperature for the non-isothermal cure of the epoxy-anhydride and heat capacity of the fully cured material at 0.2°C min^{-1}. Experimental profiles obtained with correction for dynamic C_p calibration (———) (see Section 3.9.1), calculated reference profiles for the C_p of the liquid or rubbery state, C_{pl}, and the glassy state, C_{pg} (- · · · -), and C_p profiles for single point C_p calibration (- - - -) (note the difference below −50°C).

3.5. Degree of (de)vitrification: Determination of the heat capacity-based mobility factor

The previous sections demonstrate that the evolution of the heat capacity in both isothermal and non-isothermal experiments can be used to quantify the times of vitrification and devitrification. Moreover, the influence of the heating rate indicates the importance of the level of C_p in relation to the liquid and glassy reference states. To quantify this degree of (de)vitrification, the mobility factor has been introduced [7,8].

The normalized mobility factor, DF^*, based on the heat capacity variation, was proposed in two earlier publications [7,8] and is rewritten in its general form in Eq. (1)

$$DF^*(x,T) = \frac{C_p(x,T) - C_{pg}(x,T)}{C_{pl}(x,T) - C_{pg}(x,T)} \quad (1)$$

The equation states that variations in heat capacity C_p are normalized between unity for the liquid or unrestricted state (with heat capacity C_{pl}), and zero for a frozen glassy state (with heat capacity C_{pg}) [7,8]. The evolution of this factor should mirror the reduction of mobility due to vitrification only, and not the changes in heat capacity due to changes in temperature or to the reaction itself (Section 3.4). Therefore, the

influence of both temperature and conversion on the reference states, C_{pl} and C_{pg}, needs to be taken into account to obtain quantitative results.

To incorporate the effects of both temperature and conversion in C_{pl} and C_{pg} the evolutions with temperature of C_{pl} and C_{pg} were determined for zero and full conversion. Subsequently, the evolution with conversion was assumed to be linear. This assumption is supported by a linear variation of C_p with conversion in isothermal measurements [7]. As an example, the resulting $C_{pl}(x,T)$ and $C_{pg}(x,T)$ reference lines for the cure of the epoxy-anhydride system at 0.2°C min^{-1} (Fig. 4a) are shown in Fig. 7. The effect of a dynamic heat capacity calibration is illustrated; more details are given in Section 3.9.1.

The evolution of the heat capacity-based mobility factor for the non-isothermal experiments shown in Fig. 6(a,b) are given in Fig. 8(a,b) for the epoxy-anhydride and epoxy-amine systems, respectively. For both thermosetting systems, the mobility factor increases from zero to one at T_{go} (not shown). An interval of full mobility (DF^* equal to one) follows. At certain combinations of temperature and conversion, (partial) vitrification and subsequent devitrification occur: the mobility factor first decreases, reaches a minimum, and increases again to a value of one. The transition temperatures T_{vit} and T_{devit} correspond (by definition) to a value of DF^* equal to 0.5.

In addition to the transition temperatures, DF^* gives information concerning the extent of vitrification during the diffusion-controlled or mobility-restricted cure. For the anhydride-cured system the lowest level of DF^* is 0.25 and 0.6, for a heating rate of 0.2°C min^{-1} and 0.4°C min^{-1} respectively. This indicates that the material only partially vitrifies: 25% and 60% of mobility is still available at the minimum. Because DF^* never reaches 0.5 at 0.4°C min^{-1}, one can only speak of an onset of vitrification in this case. At a rate of 0.7°C min^{-1} only a very limited amount of vitrification is observed.

In contrast, for the amine system at a heating rate of 0.2°C min^{-1}, DF^* drops immediately to a level close to zero: the material almost completely vitrifies. Even at higher heating rates up to 2.5°C min^{-1}, the level of DF^* remains below 0.2.

Considering the results of both organic systems, the impact of vitrification on the cure is much stronger for the epoxy-amine. For the epoxy-amine at the same

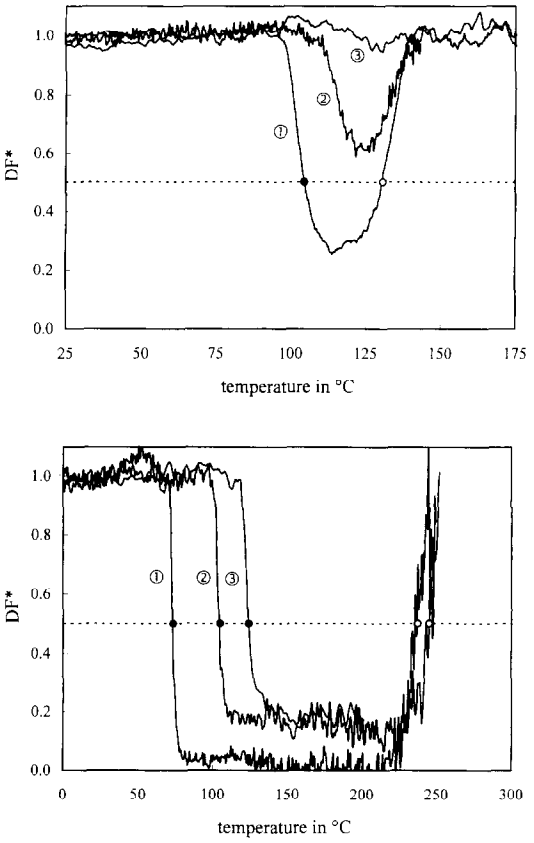

Fig. 8. (a) Evolution of the mobility factor DF^* for the non-isothermal cure of the epoxy-anhydride at (1) 0.2, (2) 0.4, and (3) 0.7°C min^{-1}. The points (●) and (○) denote the temperatures at vitrification and devitrification, respectively ($DF^* = 0.5$). (b) Evolution of the mobility factor DF^* for the non-isothermal cure of the epoxy-amine at (1) 0.2, (2) 1, and (3) 2.5°C min^{-1}. The points (●) and (○) denote the temperatures at vitrification and devitrification. respectively ($DF^* = 0.5$).

heating rate, vitrification occurs at a lower temperature and conversion, and the degree of (de)vitrification is closer to zero. The first two points are due to a higher reactivity on the one hand, and to a faster increase of T_g with conversion on the other hand. The higher degree of vitrification (the stronger decrease in mobility factor) corresponds to a bigger difference between T_g and T for the epoxy-amine than for the epoxy-anhydride (on the condition that the width of the glass transition is more or less equal for both resins). This is in accordance with the results for the isothermal experiments and is related to the reactivity and the chemical structure of the reagents, as explained in

more detail in Ref. [7]. Moreover, since $T_{g\infty}$ amounts to 255°C for the amine system, devitrification occurs at a temperature approx. 125°C above vitrification (the value depends on the heating rate, all numbers given here are for 1°C min^{-1}). The importance of this extended (heating rate-dependent) mobility-restricted cure on the final material's properties should be emphasized. For this amine-cured tetrafunctional epoxy, an increase in T_g of approx. 125°C, corresponding with a residual cure of approx. 24% and a reaction enthalpy of more than 120 J g^{-1}, happens in diffusion-controlled conditions and drastically influences the final network structure (crosslink density). An accurate quantitative description of this process is indispensable for an optimized thermoset processing.

3.6. Determination of the diffusion factor using kinetics modelling

In the previous section the heat capacity-based mobility factor was proposed and its evolution discussed. In the following sections, how this factor is related to the decrease in rate of reaction for mobility-restricted cure will be shown.

To describe the decrease in rate of reaction in diffusion-controlled conditions, a normalized diffusion factor based on heat flow, *DF*, is introduced [7,8,12,13]. It accounts for the lower rate of reaction in the vitrified state, $(dx/dt)_{obs}$, as compared to the chemical rate, $(dx/dt)_{kin}$, calculated for the same temperature and conversion using a model for the chemical kinetics in the absence of mobility control [7,8,12,13]

$$\left(\frac{dx}{dt}(x,T)\right)_{obs} = \left(\frac{dx}{dt}(x,T)\right)_{kin} \cdot DF(x,T) \quad (2)$$

The diffusion factor *DF* ranges from unity in the unrestricted state, to zero in the frozen glass (for more details see Ref. [7]). The rate of conversion, dx/dt, is obtained by normalizing the non-reversing heat flow with the total reaction enthalpy ΔH_{tot}. The conversion, x, is determined by integration of the non-reversing heat flow signal normalized by ΔH_{tot}. For each thermosetting system, a (nearly) constant value of ΔH_{tot} is taken (see Section 2.3 and Section 3.4).

To derive the diffusion factor from the normalized observed heat flow, the kinetics for the chemically controlled reaction need to be well known, especially when studying non-isothermal reactions (due to the broad temperature range covered by the non-isothermal reaction exotherm). The chemical rate of reaction can be modelled by the semi-empirical autocatalytic rate equation

$$\left(\frac{dx}{dt}(x,T)\right)_{kin} = (k_1 + k_2 x^m)(1-x)^n \quad (3)$$

with k_1 and k_2 rate constants and m and n reaction orders [31,32]. Using rate constants obeying an Arrhenius law, the equation can be used for modelling both isothermal and non-isothermal experiments.

To obtain a quantitative model describing the chemically controlled rate of reaction, the parameters in the autocatalytic rate equation (Eq. (3)) are derived using multiple isothermal and non-isothermal MTDSC and conventional DSC experiments for different temperatures and heating rates. For each experiment, a set of data points in the region *before* vitrification is withheld (this criterion can be checked easily by examining the heat capacity evolution or the mobility factor). The autocatalytic rate equation (Eq. (3)) is integrated numerically for all experiments, and the parameters are calculated by fitting *all* calculated and experimental rate of conversion versus time profiles *simultaneously*. In the integration the measured temperature–time profiles are used to allow for small deviations between sample and program temperature in a heat flux DSC. The fitting procedure results in a *single set* of four Arrhenius parameters and two reaction orders (see Eq. (3)) that can be used to calculate the evolution of conversion and rate of conversion, in the absence of mobility restrictions, for *all* temperature profiles. Considering the wide range of experimental conditions included, the agreement reached between experiment and model is very satisfactory. More details about the modelling and some experimental and optimized rate of conversion profiles are shown in Ref. [8] (see also Section 3.7).

In order to calculate the diffusion factor, *DF*, the observed rate of conversion, $(dx/dt)_{obs}$, has to be compared to the chemical rate, $(dx/dt)_{kin}$, calculated for the same conversion and temperature (Eq. (2)). The evolution of both rates is given in Fig. 9(a,b) for an isothermal and a non-isothermal epoxy-anhydride cure, respectively. For each point in time or temperature, $(dx/dt)_{kin}$ is calculated using the kinetic model with optimized parameters (Eq. (3)) and for the

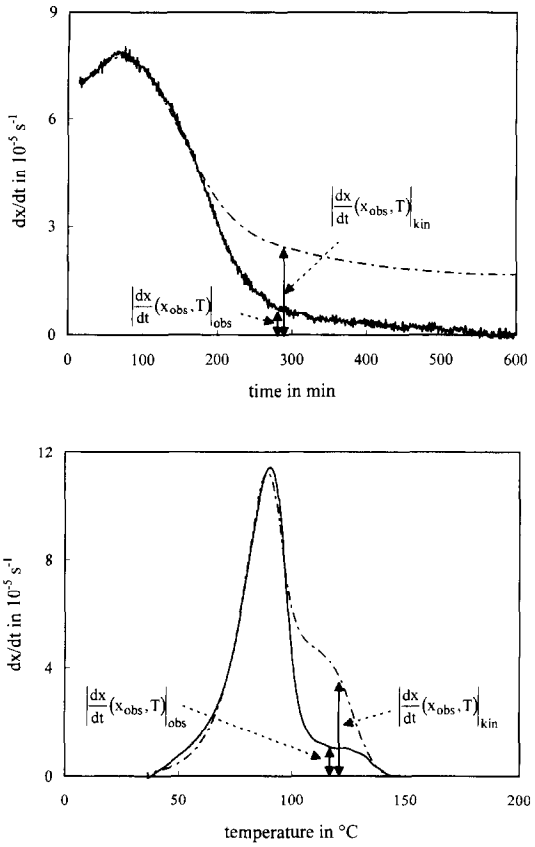

Fig. 9. (a) Rate of conversion versus reaction time for the cure of the epoxy-anhydride at 80°C. Experimental rate $(dx/dt)_{obs}$ (———) and rate expected for the same conversion in the absence of mobility restrictions, $(dx/dt)_{kin}$ (- · - · -). (b) Rate of conversion versus reaction temperature for the cure of the epoxy-anhydride at 0.2°C min^{-1}. Experimental rate $(dx/dt)_{obs}$ (———) and rate expected for the same conversion and temperature in the absence of mobility restrictions, $(dx/dt)_{kin}$ (- · - · -). [8].

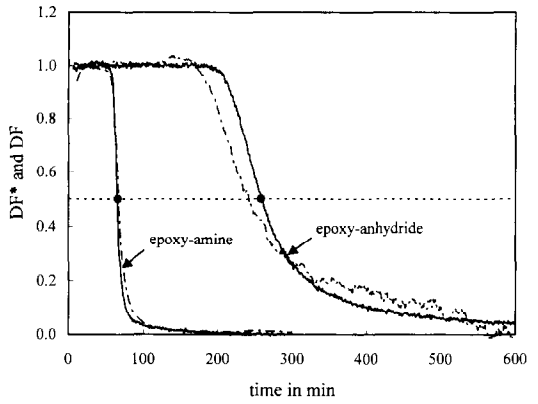

Fig. 10. Comparison of the mobility factor DF^* based on heat capacity (———) and the diffusion factor DF based on non-reversing heat flow (- · - · -) for the cure of the epoxy-anhydride and epoxy-amine systems at 80°C. The points (●) denote the time at vitrification ($DF^* = 0.5$).

experimental conversion and temperature corresponding to that point.

3.7. *Comparison of diffusion and mobility factors for the thermosetting systems*

The isothermal and non-isothermal evolutions of the diffusion and mobility factors, deduced from non-reversing heat flow and heat capacity as outlined in the previous sections, are compared in Figs. 10 and 11(a,b) for both epoxy systems. Similar results for other experimental conditions can be found in Refs. [7,8].

For isothermal measurements the two factors, originating from two different experimental quantities, give quantitatively the same evolution and almost coincide; this observation is valid for both epoxy systems (Fig. 10). For non-isothermal experiments (Fig. 11(a,b)) the diffusion factor DF can only be determined when the non-reversing heat flow due to reaction (or the rate of reaction) is sufficiently high. To the contrary, the mobility factor DF^* can be given for the entire temperature range, since it is calculated directly from the measured heat capacity and the reference lines C_{pl} and C_{pg}. Limited deviations of the heat flow diffusion factor are seen before vitrification and after devitrification (Fig. 11(a,b)). The first reason is that the kinetic model does not perfectly fit the observed rate of conversion profile, leading, for example, to values higher than unity for DF. One should bear in mind that the parameters are optimized for multiple experiments, which results in a model that is valid for a wide range of conditions, but also in a somewhat lesser fit for the individual experiments. The second source of error for DF is the small rate of conversion at the start and end of the reaction exotherm. When the heat flow is almost zero, small deviations lead to big errors in DF.

In the temperature range between vitrification and devitrification, the agreement is very good: for the epoxy-anhydride resin, both factors give quantitatively the same results concerning the temperature

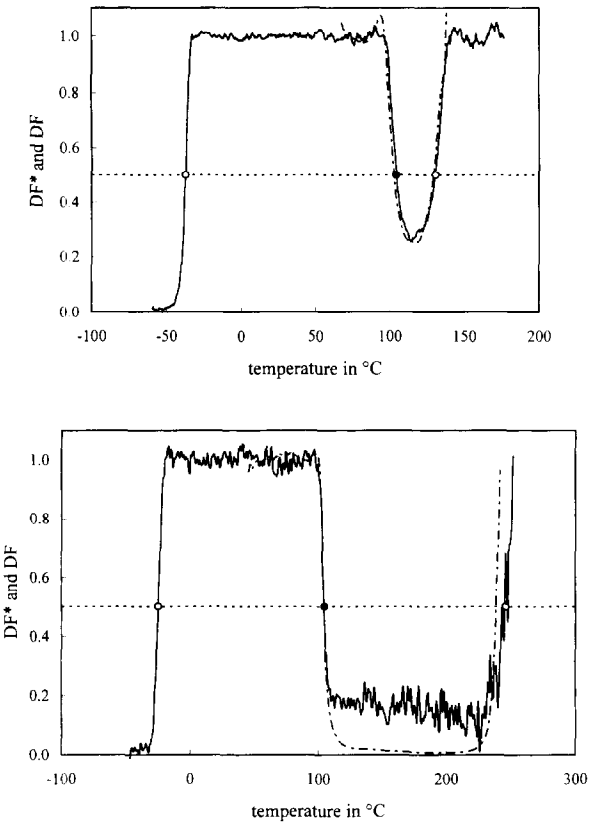

Fig. 11. (a) Comparison of the mobility factor DF^* based on heat capacity (———) and the diffusion factor DF based on non-reversing heat flow (- · · · -) for the cure of the epoxy-anhydride at 0.2°C min^{-1}. The points (●) and (○) denote the temperatures at vitrification and devitrification, respectively ($DF^* = 0.5$). (b) Comparison of the mobility factor DF^* based on heat capacity (———) and the diffusion factor DF based on non-reversing heat flow (- · · · -) for the cure of the epoxy-amine at 1°C min^{-1}. The points (●) and (○) denote the temperatures at vitrification and devitrification, respectively ($DF^* = 0.5$).

and the mode of decrease (vitrification) and increase (devitrification), as well as the degree of vitrification reached in between (Fig. 11(a)). For the amine-epoxy the level reached in between vitrification and devitrification is higher for DF^* than for DF (Fig. 11(b)). This deviation is probably (partly) due to the simple kinetic model used. For correctly calculating DF, the kinetic model has to describe the reaction kinetics over the entire range covered by the reaction exotherm. For the epoxy-amine this temperature interval ranges from 25°C to 250°C, which is much wider than for the epoxy-anhydride system (25°C to 150°C). Moreover, performing experiments in chemically controlled conditions at elevated temperatures (above 150°C) is impossible for the highly reactive amine system (the heating rate needed is too fast). Thus, the kinetic model is optimized for the first half of the temperature interval only, leading to larger deviations at higher temperatures. In addition, primary and secondary amine functionalities with different reactivities are present in the reacting system [13,14]. This is not accounted for by the empirical model (Eq. (3)). By incorporating this different reactivity in the reaction model, using a more mechanistic approach of the chemical kinetics, the deviations could probably be reduced further (future work). Note that the agreement between DF and DF^* is much better for lower heating rates (e.g. 0.2°C min^{-1} [8]).

In general, the diffusion factor and mobility factor coincide very well in almost all experimental conditions for both epoxy resins. Only small deviations occur for the amine system at higher heating rates, probably due to a less efficient kinetic modelling. So, the evolution of the normalized heat capacity gives a direct indication on isothermal and non-isothermal diffusion-controlled cure. Therefore the evolution of DF^* can be used to evaluate theoretical models for diffusion control. Moreover, in conditions of very slow reactions where the heat flow cannot be measured quantitatively, the changes in heat capacity and DF^* can still be determined accurately, and the deceleration of the reaction rate can be followed quantitatively, in a single MTDSC experiment.

3.8. *The influence of chemistry on the (de)vitrification process*

For the inorganic polymer glass the diffusion factor DF and the mobility factor DF^* were calculated using the same procedures as for the organic resins. The comparison of their evolution is made in Fig. 12. For this inorganic system the diffusion factor DF stays near unity long after the decrease of the mobility factor DF^* : DF^* has decreased by 90% before DF also starts decreasing. Vitrification, defined as half of the decrease in heat capacity, occurs at low conversion, while the reaction rate is still near its maximum, but as opposed to observations for the organic resins, no marked decrease in the rate of reaction is observed

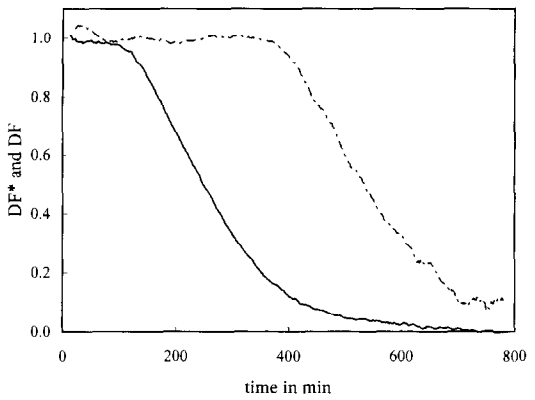

Fig. 12. Comparison of the mobility factor DF^* based on heat capacity (———) and the diffusion factor DF based on non-reversing heat flow (- · - · -) for the isothermal reaction of the inorganic polymer glass at 35°C.

at that time. The conversion increases another 30% before the end of the reaction exotherm. A glass transition temperature of at least 175°C is reached for an isothermal cure at 35°C. In addition it is impossible to measure T_g for intermediate conversions: in a subsequent heating of a partially reacted sample the residual exotherm starts before a glass transition is seen. All these facts are intrinsically in accordance with a reaction continuing in the vitrified state. After polymerization and elimination of free water, T_g is around 650°C [10].

On a molecular scale, the glass transition in inorganic polymer networks differs quite strongly from the transition in organic polymers: it is a chemical process, corresponding to an equilibrium of bond breaking and formation, enabling reorganizations to take place [10,33,34]. The reaction of metakaolinite and sodium silicate solution to a network of SiO_4 and AlO_4 tetrahedra in which no Al–O–Al bonds occur [9], is probably a short-range reorganization, not involving the movement (translational diffusion) of large entities. Small molecules and ions (H_2O, OH^-, Na^+) are known to play an important role in the reaction mechanism [9,10]. The results indicate that the reaction is not impeded upon vitrification of the material, hence the transition from a liquid to a glass is not a physical barrier for the low-temperature cure of this inorganic material. The reaction continues until mobility on a smaller molecular scale is restricted.

Anyway, the fact that the diffusion and mobility factors do not coincide for the IPG indicates that care has to be taken when using the experimentally determined mobility factor to predict the rate of reaction of a material in conditions of mobility control. When the molecular motions frozen out at vitrification do not correspond to the molecular motions needed for reaction, the mobility and the diffusion factor will be shifted in time. If mobility limitations on the rate of reaction only become important when mobility is restricted on a smaller molecular scale than the motions constrained at vitrification, the heat flow diffusion factor DF will be shifted toward higher conversions as compared to the mobility factor DF^*.

3.9. Considerations regarding MTDSC for studying thermosetting systems

3.9.1. Dynamic heat capacity calibration

For all experiments the heat capacity signal was calibrated at a single point (see Section 2.3). The experimental error on heat capacity can further be reduced by dynamic calibration over the entire temperature range instead of at a single temperature. To check the evolution of the heat capacity calibration constant, K_{C_p}, over the entire temperature range, the heat capacity of a 23 mg sapphire standard (TA Instruments) was measured from −150°C to 300°C at 2.5°C min^{-1} with a 0.5°C per 60 s modulation. Comparison with literature values [35] showed a gradual evolution of K_{C_p} with a total variation of 5% between −50°C and 300°C Below −50°C the deviation increases.

The effect of the dynamic heat capacity calibration on the evolution of the heat capacity itself is shown in Fig. 7. Using dynamic calibration much of the curvature disappears, and heat capacity increases more or less linearly with temperature. For the results of this work, this correction is not so important: when calculating DF^*, the heat capacity is normalized to reference heat capacities determined at the same temperature and thus changes in K_{C_p} have almost no effect on the results.

3.9.2. Non-reversing heat flow versus conventional DSC heat flow

The non-reversing heat flow obtained in isothermal MTDSC experiments agrees very well with the heat

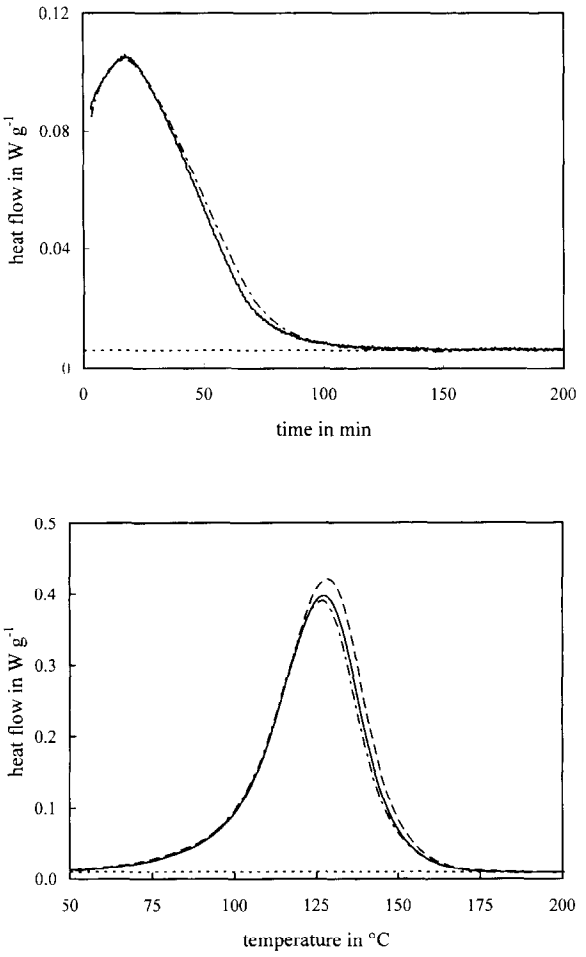

Fig. 13. (a) Comparison of the non-reversing heat flow obtained in MTDSC (———) to the heat flow obtained in conventional DSC (- - - -) for the isothermal cure of the epoxy-anhydride at 100°C. (b) Comparison of the non-reversing heat flow obtained in MTDSC programmed at 2.5°C min^{-1} (———) to the heat flow obtained in conventional DSC at 2.5°C min^{-1} (- - - -) and at 2.3°C min^{-1} (- · - · -) for the non-isothermal cure of the epoxy-anhydride.

flow evolution obtained in a conventional DSC experiment, performed under the same conditions with exception of the modulation (Fig. 13(a)). Neither changing the modulation amplitude nor the period had an effect on the reaction exotherm seen in the non-reversing heat flow. These results indicate that the temperature modulation does not affect (or to a negligible extent) the reaction kinetics.

Also in non-isothermal conditions, the chemical rate of reaction can be obtained quantitatively from the non-reversing heat flow. In principle, for a correct calculation of the non-reversing heat flow in non-isothermal experiments, attention has to be paid to the heat capacity and heating rate used for obtaining the reversing heat flow. Firstly, the dynamic heat capacity should be used in order to correct for the temperature dependence of K_{C_p} (see Section 3.9.1). However, for the curing experiments shown in this work the gradual change in K_{C_p} (when using a dynamic calibration instead of a single point calibration) results only in minor baseline variations for the reaction exotherm in the non-reversing heat flow. Secondly, one should use the measured underlying heating rate to correctly subtract the heat capacity contribution (reversing heat flow) from the total heat flow, instead of using the programmed heating rate to calculate the reversing heat flow, as currently implemented in the commercial software (TA Instruments). For a programme heating rate of 2.5°C min^{-1}, an experimental heating rate of approx. 2.3°C min^{-1}, or a 5 to 10% difference, was obtained over the entire temperature range (in conventional experiments on the same apparatus the difference is much smaller). When an important contribution of the reversing heat flow to the total heat flow is plausible, for example, in the melting region of semi-crystalline polymers, the correction on the reversing heat flow becomes quite important. However, in the cure experiments shown here, the effect of this second correction on the non-reversing heat flow is always small because the contribution of the change in the reversing heat flow is small compared to the non-reversing heat flow. Besides, the corrections are generally much smaller than the experimental error which is due to small differences in the mixing ratios (a new epoxy-hardener mixture is made for each experiment) and the influence of small (irreproducible) amounts of moisture on the reaction kinetics.

The deviation of the measured heating rate from the programmed heating rate plays an important role when studying the chemical kinetics. When comparing conventional and modulated DSC experiments, the correct *experimental* heating rates must be used. As can be seen in Fig. 13(b), the modulated DSC curve (programmed 2.5°C min^{-1}; measured approx. 2.3°Cmin^{-1}) agrees better with the conventional DSC curve at a programmed (and experimental) heating rate of 2.3°C min^{-1} than if 2.5°Cmin^{-1}.

Consequently, when modelling the chemical kinetics, the measured temperature (and hence the measured heating rate) should be used for interpreting the experimental results (see also Section 3.6).

Note that not all non-isothermal experiments were performed using 'heating only' conditions. This is not necessary for a correct and quantitative interpretation of the results.

Note also that the comparison made between MTDSC and conventional DSC is performed on a TA Instruments 2920 DSC equipped with the MDSC™ accessory. In principle, the same conclusions are valid on other MTDSC devices (see also Section 3.9.3).

3.9.3. *Heat flow phase and related signals: 'Complete' versus 'simple' deconvolution*

In many thermal analysis techniques that use an oscillating excitation of the material, for example, dynamic mechanical analysis, torsional braid analysis, dielectric thermal analysis, and dynamic rheometry, a phase angle is defined between the 'modulated' input and the resulting output signal. A similar approach can be used for MTDSC [4,36,37]. The heat flow phase is defined as the phase angle of the modulated heat flow output (with the convention of a negative heat flow for exothermic events) with respect to the modulated heating rate input. The heat flow phase can be corrected for the instrument contribution by shifting the curve to the zero level for reference points where no transition occurs [4,6,37].

For the epoxy-anhydride cure at 80°C (Fig. 2), the heat flow phase measured isothermally at 80°C for the fully cured resin after residual non-isothermal curing, was used as a reference point (−29°). Thus, the correction (shift) applied to the curve equals +29°. The corrected heat flow phase, ϕ, initially amounts to −2.0° (Fig. 14(a)). As the reaction proceeds ϕ slowly evolves toward zero. A (downward) local extreme is observed at 247 min and corresponds to the vitrification transition. At the end of the isothermal experiment ϕ equals −0.6°.

The evolution of the corrected heat flow phase for the first and second heating of the epoxy-anhydride system at 0.2°C min^{-1} is depicted in Fig. 14(b). The points at −75°C (−32°) and 80°C(−31°) for the fully cured resin (second heating) were chosen as reference points for the instrument phase correction, and thus

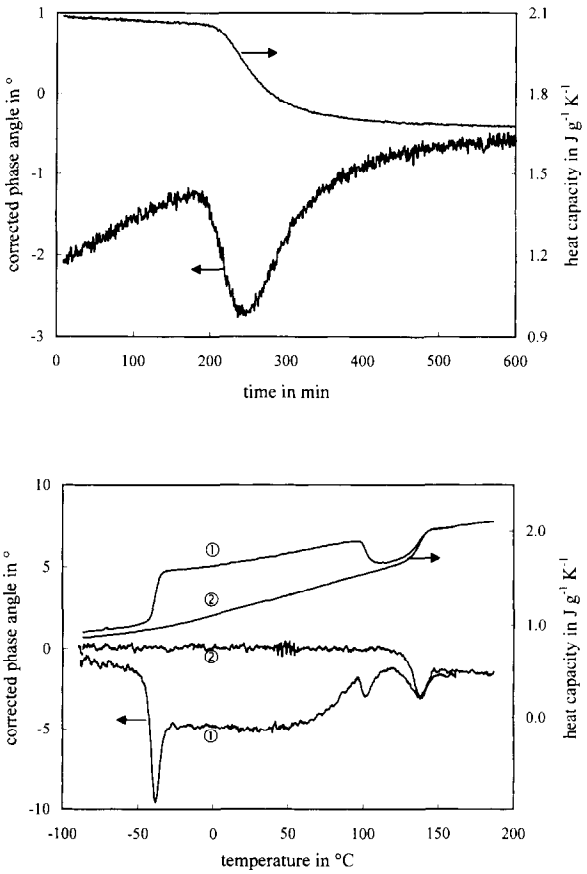

Fig. 14. (a) Corrected heat flow phase and heat capacity for the quasi-isothermal cure of the epoxy-anhydride at 80°C. (b) Corrected heat flow phase and heat capacity for the non-isothermal cure of the epoxy-anhydride ((1)) and for the fully cured material ((2)), at 0.2°C min^{-1}.

were shifted to zero. In the first heating, three (downward) local extremes can be observed at −38°C, 101°C, and 138°C. These extremes coincide with, respectively, initial devitrification, vitrification, and devitrification, as observed by comparison with the heat capacity evolution. During the reaction, ϕ slowly evolves toward zero as the reaction proceeds. In the second heating ϕ stays close to zero with only one extreme at 138°C corresponding to the glass transition of the fully cured system.

Using the corrected phase angle and the modulus of the complex heat capacity, $|C|$, which is the ratio of the amplitudes of heat flow output over the heating rate input, the components in-phase (C') and out-of-phase

(C'') with the modulated heating rate can be calculated using Eq. (4) (for more detailed approaches see Refs. [4,36,37]).

$$C' = |C| \cdot \cos\phi$$

$$C'' = -|C| \cdot \sin\phi \tag{4}$$

$$|C| = \sqrt{(C')^2 + (C'')^2} = \left(\frac{A_{HF}}{A_T \cdot \omega}\right)$$

The in-phase component C' corresponds to the thermodynamic heat capacity [36,37]. The out-of-phase component C'' is linked to kinetic events [37]. For the systems and conditions studied in this work, the heat flow phase always remains small during the course of the reaction: the maximum difference with respect to the reference state is 5° (10° at T_{go}). The cosine and sine for this angle equal 0.996 and 0.09 respectively. Thus, for all experiments shown, C' and $|C|$ coincide within 0.4%, and C'' is always close to zero. This implies that the reversing and non-reversing heat flows calculated using C' (approach called 'complete deconvolution') or $|C|$ (approach called 'simple deconvolution') are virtually identical. Hence, the use of the phase angle is not necessary for the quantitative interpretation of the results presented here. All the non-reversing heat flow curves shown were obtained with the simple deconvolution.

At this instant, more results are needed for a thorough discussion of the evolution of the heat flow phase during the cure of thermosetting systems. Nevertheless, the preliminary results presented in this work already point to a relation between phenomena observed in the heat flow phase and the cure, vitrification, and devitrification of the thermosetting systems. This indicates that the heat flow phase signal contains valuable 'chemo-rheological' information. This additional MTDSC information will be elaborated in future work.

When the 'complete deconvolution' is used, resulting in in-phase and out-of-phase components, the modulated DSC approach (TA Instruments MDSC), based on Fourier deconvolution, is completely equivalent to the dynamic DSC approach (Perkin–Elmer DDSC) which is based on the linear response theory [36]. Results for non-isothermal cure experiments confirm the equivalency of both techniques. However, in order to be able to obtain quantitative results with the DDSC device for isothermal curing conditions, the current software implementation of DDSC has to be adapted.

4. Conclusions

The results obtained indicate that MTDSC is a very useful technique for studying the cure behaviour of thermosetting systems both in isothermal and non-isothermal conditions. Using a single MTDSC experiment, vitrification and devitrification can be observed as step changes in the heat capacity signal, while at the same time the evolution of the reaction rate is followed in the non-reversing heat flow signal. The information available in the heat capacity evolution is a key factor for the correct interpretation of the heat flow signal. First results indicate that the heat flow phase angle contains interesting information regarding the rheological state of the reacting material.

A mobility factor based on heat capacity, DF^*, is proposed in this work. For both epoxy resins studied, it was shown that the points for which DF^* equals 0.5 can be used to quantify the times and temperatures of vitrification and devitrification. Moreover, the DF^* curve gives information on the degree of vitrification while the reaction occurs in mobility-restricted conditions.

The mobility factor based on the heat capacity coincides very well with the diffusion factor, calculated from the non-reversing heat flow via chemical kinetics modelling, and describing the effects of diffusion control on the rate of conversion of the cure reaction. Although the two resins behave quite differently, this coincidence between the mobility factor and diffusion factor is valid for both systems. Therefore, the mobility factor can be used for a quantitative description of their altered rate of conversion in the (partially) vitrified state: for the decrease in the rate during the vitrification, the increase in the rate during devitrification, and the diffusion-controlled rate in the (partially) vitrified region in between both processes.

The formation of an inorganic polymer glass is (nearly) uninfluenced by vitrification: the rate of reaction only decreases at the end of the vitrification process, and a glass transition temperature largely above the cure temperature is reached. This is attributed to reactions requiring less mobility than the

mobility frozen out at vitrification; the mobility needed for the reaction is only frozen out long after vitrification occurred.

Using both isothermal and non-isothermal MTDSC experiments, the effects of polymer structure and reaction mechanism on the (partially vitrified) cure reaction could be studied in more detail, theoretical models for diffusion control could be evaluated, and improved processing conditions for thermosetting resins could further be developed with temperature–time transformation (TTT) and continuous-heating transformation (CHT) diagrams [30].

Acknowledgements

The work of G. Van Assche and A. Van Hemelrijck was supported by grants from the Flemish Institute for the Promotion of Scientific-Technological Research in Industry (I.W.T.).

References

[1] M.J. Richardson, in V.B.F. Mathot, Calorimetry and Thermal Analysis of Polymers, Hanser, Munich, 1994, pp. 169, 189.
[2] M. Reading, A. Luget and R. Wilson, Thermochim. Acta, 238 (1994) 295.
[3] B. Wunderlich, Y. Jin and A. Boller, Thermochim. Acta, 238 (1994) 277.
[4] M. Reading, Trends in Polymer Sci., 1 (1993) 248.
[5] P.S. Gill, S.R. Sauerbrunn and M. Reading, J. Therm. Anal., 40 (1993) 931.
[6] M. Reading, D. Elliot and V.L. Hill, J. Therm. Anal., 40 (1993) 949.
[7] G. Van Assche, A. Van Hemelrijck, H. Rahier and B. Van Mele, Thermochim. Acta, 268 (1995) 121.
[8] G. Van Assche, A. Van Hemelrijck, H. Rahier and B. Van Mele, Thermochim. Acta, 286 (1996) 209.
[9] H. Rahier, B. Van Mele, M. Biesemans, J. Wastiels and X. Wu, J. Mater. Sci., 31 (1996) 71.
[10] H. Rahier, B. Van Mele and J. Wastiels, J. Mater. Sci., 31 (1996) 80.
[11] S. Montserrat, J. Appl. Polym. Sci., 44 (1992) 545.
[12] H. Stutz, J. Mertes and K. Nuebecker, J. Polym. Sci. Part A: Polym. Chem., 31 (1993) 1879.
[13] G. Wisanrakkit and J.K. Gillham, J. Coat. Technol., 62 (1990) 35.
[14] G. Wisanrakkit and J.K. Gillham, J. Appl. Polym. Sci., 42 (1991) 2453.
[15] J.K. Gillham and J.B. Enns, Trends in Polymer Sci., 2 (1994) 406.
[16] M.T. Aronhime and J.K. Gillham, Adv. Polym. Sci., 78 (1986) 83.
[17] X. Wang and J.K. Gillham, J. Appl. Polym. Sci., 47 (1993) 425.
[18] M.G. Parthun and G.P. Johari, Macromolecules, 25 (1992) 3149.
[19] K.A. Nass and J.C. Seferis, Polym. Eng. Sci., 29(5) (1989) 315.
[20] S.D. Senturia and N.F. Sheppard Jr., Adv. Polym. Sci., 80 (1986) 1.
[21] H.H. Winter, Polym. Eng. Sci., 27 (1987) 1698.
[22] A.Ya. Malkin and S.G. Kulichikhin, Adv. Polym. Sci., 101 (1992) 217.
[23] J.B. Enns and J.K. Gillham, J. Appl. Polym. Sci., 28 (1983) 2567.
[24] M. Cassettari, G. Salvetti, E. Tombari, S. Veronesi and G.P. Johari, J. Polym. Sci. Part B: Polym. Phys., 31 (1993) 199.
[25] M. Cassettari, F. Papucci, G. Salvetti, E. Tombari, S. Veronesi and G.P. Johari, Rev. Sci. Instrum., 64 (1993) 1076.
[26] National Institute of Standards and Technology, Standard Reference Materials Program, SRM 1475 – Linear Polyethylene, Gaithersburg, 1993.
[27] V.B.F. Mathot and M.F.J. Pijpers, J. Therm. Anal., 28 (1983) 349.
[28] R.A. Robie and B.S. Hemingway, Clays and Clay Minerals, 39 (1991) 362.
[29] S. Montserrat, Polymer, 36(2) (1995) 435.
[30] A. Van Hemelrijck, G. Van Assche and B. Van Mele, in preparation.
[31] M.R. Kamal, Polym. Eng. Sci., 14 (1974) 231.
[32] S. Montserrat and J. Málek, Thermochim. Acta, 228 (1993) 47.
[33] J.M. Jewell, C.M. Shaw and J.E. Shelby, J. Non-Cryst. Solids, 152 (1993) 32.
[34] O.V. Mazurin, J. Non-Cryst. Solids, 129 (1991) 259.
[35] D.A. Ditmars, S. Ishihara, S.S. Chang, G. Bernstein and E.D. West, J. Res. Nat. Bur. Stand., 87(2) (1982) 159.
[36] J.E.K. Schawe, Thermochim. Acta, 261 (1995) 183.
[37] A.A. Lacey, C. Nikolopoulos and M. Reading, submitted to J. Therm. Anal.